

In vitro study of the proliferation and growth of human bone marrow cells on apatite–wollastonite–2M glass ceramics

M. Magallanes-Perdomo^a, A.H. De Aza^{a,*}, A.Y. Mateus^{b,c}, S. Teixeira^{b,c}, F.J. Monteiro^{b,c}, S. De Aza^a, P. Pena^a

^a Instituto de Cerámica y Vidrio, CSIC, C/Kelsen 5, 28049 Madrid, Spain

^b Laboratório de Biomateriais, INEB-Instituto de Engenharia Biomédica, Rua do Campo Alegre 823, 4150-180 Porto, Portugal

^c Departamento de Engenharia Metalúrgica e de Materiais, FEUP, Rua Dr Roberto Frias s/n, 4200-465 Porto, Portugal

ARTICLE INFO

Article history:

Received 10 August 2009

Received in revised form 10 December 2009

Accepted 14 December 2009

Available online 21 December 2009

Keywords:

Glass ceramics

Cell culture

Apatite

Wollastonite

Cell proliferation

ABSTRACT

This study concerns the preparation and in vitro characterization of an apatite–wollastonite–2M bioactive glass ceramic which is intended to be used for the regeneration of hard tissue (i.e. in dental and cranio-maxillofacial surgery). This bioglass ceramic has been obtained by appropriate thermal treatment through the devitrification (crystallization) of a glass with a stoichiometric eutectic composition within the $\text{Ca}_3(\text{PO}_4)_2$ – CaSiO_3 binary system. Crack-free specimens of the bioglass ceramic were immersed in human bone marrow cell cultures for 3, 7, 14 and 21 days, in order to study biocompatibility. Cell morphology, proliferation and colonization were assessed by scanning electron microscopy and confocal laser scanning microscopy. A total protein content assay was used to evaluate the viability and proliferation of cultured bone marrow cells. The results showed that the cells were able to adhere and proliferate on the designed material due to the essentiality of silicon and calcium as accessory factors for cell activity stimulation.

© 2009 Acta Materialia Inc. Published by Elsevier Ltd. All rights reserved.

1. Introduction

A series of calcium phosphate-based biomaterials, including different bioglasses, glass ceramics, ceramics, cements, coatings and bioactive composites, have been developed for hard tissue repair due to their biocompatibility and osteoconductivity, as has been reported elsewhere [1–6]. On the other hand, silicon has received attention as a substitute in calcium phosphates crystalline networks for biomaterials because it plays an essential role in the metabolic events that induce new bone formation [7,8]. It has been shown that silicon is localized in active growth areas such as the osteoid of the bone of young mice and rats [7,8]. Furthermore, it was found that insufficient silicon intake in rats resulted in disturbances in the development of bone structures, in terms of skull size and bone architecture, and also retarded normal bone growth [7,8]. Additionally, Reffitt et al. [9] demonstrated that orthosilicic acid present in physiological concentrations (5–20 mM) stimulated collagen type I synthesis and enhanced osteoblast differentiation, while treatment at a higher concentration resulted in only a small increase in collagen synthesis. Thus, silicon is essential for the growth and development of certain biological tissues, such as bone, teeth and some invertebrate skeletons.

Furthermore, a recent work [10] on the mechanisms behind the bioactivity of pseudo-wollastonite (psW) (α - CaSiO_3) showed a sup-

plementary beneficial effect that co-treatment with silicon and calcium has on bone cell activity stimulation, compared with treatments with either element separately.

According to the above considerations, materials containing phosphorus, calcium and silicon are promising candidates for preparing bioceramics and glass ceramics with improved osteogenic properties. Many materials have been developed containing these elements [1–4,11–14]. One of them is the bioceramic Bioeutectic[®] [14–16]. This material is composed of two phases, psW and α -tricalcium phosphate (α -TCP) [α - $\text{Ca}_3(\text{PO}_4)_2$] and has the ability to restructure its morphology during exposure to simulated body fluid (SBF) [17] or human parotid saliva [18], by dissolution of the psW phase and subsequent pseudomorphic transformation of α -TCP into hydroxyapatite (HA). In vitro studies carried out in a dynamic flow of SBF showed that the entire psW– α -TCP dense ceramic transformed into a porous apatite phase over time [19]. Thus, this Bioeutectic[®] ceramic is a bioactive material which is totally replaced by HA in SBF [19]. As expected, it behaves similarly in in vivo experiments, facilitating the osteointegration of implants [15–20]. Unfortunately, the procedure used for the synthesis of these TCP–wollastonite (W) (CaSiO_3) potential implants, controlled slow solidification, restricts their size and even their shape [14,21].

In previous works [22,23] some of the present authors proposed glass ceramic processing to solve these problems. In these studies the mechanism of devitrification of a W–TCP eutectic glass was determined. Based on this information, it was possible to obtain a wide range of bioglass ceramics from a eutectic W–TCP binary

* Corresponding author. Tel.: +34 91 735 58 64; fax: +34 91 735 58 43.

E-mail address: aaza@icv.csic.es (A.H. De Aza).

system, with different crystalline phases present, through appropriate design of the thermal treatments.

Aimed at obtaining a biomaterial that once implanted helps the body to heal itself, the glass ceramic studied in the present work was designed and obtained by devitrification of a bulk TCP–W eutectic glass. The material obtained combines the properties of a resorbable Si/Ca-rich glass, of bioactive wollastonite (CaSiO₃-2M) and of hydroxyapatite.

The present investigation has focused on the study of the biocompatibility of the designed apatite–wollastonite-2M glass ceramic, which contains 44.8 wt.% apatite, 28.0 wt.% wollastonite-2M and 27.2 wt.% amorphous phase. The biological response of human bone marrow stem cells (HBMSCs), derived from primary cultures, to the samples was evaluated using a standardized protocol for 3, 7, 14 and 21 days. Cell morphology, adhesion and proliferation were studied by means of scanning electron microscopy (SEM) and confocal laser scanning microscopy (CLSM). Total protein content determinations were also performed. The results show that the material presents favorable conditions to support cell adhesion and proliferation.

2. Materials and methods

2.1. Sample preparation

To obtain the glass ceramic it was firstly necessary to prepare the eutectic W–TCP glass within the W–TCP system. A eutectic composition was selected because it represents the composition with the lowest melting temperature of the binary system (1402 ± 2 °C) [24].

The chemicals used for synthesis of the eutectic glass ceramic were reagent grade calcium carbonate (Merck, Darmstadt, Germany), high purity amorphous silicon (IV) oxide (100 mesh, 99.7 wt.%, Strem Chemicals, Newburyport, MA) and high purity synthetic Ca₃(PO₄)₂, whose characteristics have been reported previously [23].

The thoroughly mixed batch was melted in a Pt–10 wt.% Rh crucible at 1600 °C in an electric furnace for 30 min to ensure a homogeneous liquid and avoid the loss of volatile substances. The melt was poured at room temperature onto preheated brass molds, giving a homogeneous, bubble-free and transparent bulk glass. This was subsequently annealed close to the glass transition temperature ($T = 795$ °C for 10 min) to relieve the internal stresses [23]. Next, the glass was cut with a low speed saw (Buehler, Lake Bluff, IL) in order to obtain samples with the dimensions 3.5 × 3.5 × 3.5 mm.

The glass ceramic studied in the present work was obtained by devitrification of these bulk W–TCP eutectic glass specimens. Taking into account the previously obtained results concerning devitrification of this specific glass [22,23], a crack-free apatite–wollastonite-2M glass ceramic was obtained through the following procedure. The samples were loaded into small platinum foil crucibles and then heated in air at 5 °C min⁻¹ up to 820 °C, holding this temperature for 2 h. Then specimens were heated at 1 °C min⁻¹ up to 1100 °C, maintaining this temperature for 1 h. Subsequently the samples were cooled to 790 °C at 1 °C min⁻¹, and then at 5 °C min⁻¹ to room temperature.

2.2. Characterization of the prepared samples

2.2.1. Chemical analysis

The eutectic glass ceramic was analyzed by X-ray fluorescence (XRF) analysis to verify the stoichiometric eutectic composition of the sample. A MagiX Super Q version 3.0 Phillips X-ray fluorescence spectrometer (Phillips, The Netherlands) was used. This spec-

trometer is equipped with IQ⁺ analytical software used for qualitative and semi-quantitative analysis. Calibration curves were fitted from certified standards consisting of natural and synthetic calcium phosphates and calcium silicates.

For XRF analysis glass ceramic samples and standards were prepared as glass beads by lithium tetraborate fusion in a Perl'x2 machine (Phillips, Netherlands). The powdered sample (0.3 g) and the flux (5.5 g Li₂B₄O₇) were mixed and heated in a Pt–5 wt.% Au crucible at 1100 °C. The molten mixture was cast as an amorphous glass bead suitable for analysis.

2.2.2. X-ray diffraction (XRD)

Crystalline phases present in the glass ceramic sample were quantitatively identified by XRD analysis at room temperature and to determine the percentages of the different phases present in the sample the Rietveld method [25] was used. A tungsten carbide mill was used to grind a significant amount of glass ceramic to less than 63 μm, which was then mixed with CaF₂ as an internal standard. The final mixture contained 70.0 wt.% glass ceramic and 30.0 wt.% CaF₂.

XRD patterns were recorded on a Siemens D5000 automated diffractometer (Karlsruhe, Germany) using Cu K_{α1,2} radiation (1.5418 Å) and a secondary curved graphite monochromator. Data were collected in Bragg–Brentano ($\theta/2\theta$) vertical geometry (flat reflection mode) between 2° and 70° (2θ) in 0.03° steps, counting for 20 s per step. The sample was rotated at 0.25 s⁻¹ during the acquisition of patterns in order to improve powder averaging, which is essential to obtain accurate intensities and, hence, phase analyses. The diffractometer optics comprised a system of primary Soller foils between the X-ray tube and the fixed aperture slit. The fixed aperture of the scattering slit used was 2 mm, followed by a system of secondary Soller slits and a detector slit of 0.2 mm. The X-ray tube was operated at 40 kV at 30 mA. EVA version 6.0 Diffrac Plus software (Bruker, Karlsruhe, Germany) was used to evaluate the obtained patterns. The powder pattern obtained was refined by the Rietveld method with the GSAS program suite [26] (<http://www.ncnr.nist.gov/programs/crystallography/software/gsas.html>) using a pseudo-Voigt peak shape function, with the asymmetry correction of Finger et al. included [27]. The crystal structures used to calculate the powder patterns are given in Table 1. The related anisotropic vibration temperatures factors were converted to the corresponding isotropic values. The optimized parameters were zero shift error, cell parameters, background coefficients, peak shape parameters, preferred orientation and phase fractions.

2.2.3. Microstructural studies

After thermal treatment the specimens were mounted in epoxy resin. Then the mounted samples were polished using different grades of diamond down to 1 μm roughness. A cerium suspension was used in the final preparation when necessary. To uncover the microstructure the samples were etched with 5 vol.% acetic acid for 1 s. The microstructures of the polished and silver coated surfaces of the samples were studied by field emission scanning electron microscopy (FE-SEM) (Hitachi-S4700, Tokyo, Japan) with energy dispersive X-ray spectroscopy (EDS). Individual phases were analyzed using the Noran System Six-Thermo Electron Corporation EDS (Waltham, MA).

Table 1

Crystal structures used to calculate the powder patterns in the Rietveld analyses.

No	Code	Name	Formula	Ref.
1	152190	Ca-deficient apatite	Ca _{9.303} (PO ₄) ₆ (OH) _{0.696} 1.97(H ₂ O)	[28,29]
2	34908	Wollastonite-2M	CaSiO ₃	[30,31]

2.3. In vitro test with cell culture

2.3.1. Cell culture procedures

HBMSCs were obtained from patients undergoing orthopedic surgical procedures. Informed consent to use this biological material, that would otherwise be discarded, was obtained.

HBMSCs were thawed and then cultured in 75 cm² flasks containing 10 ml culture medium (α -minimum essential medium (α -MEM) (Gibco), 10% fetal calf serum (FCS) (Gibco), 1 vol.% fungizone (Gibco), 1 vol.% penicillin/streptomycin (Gibco)). Cells were maintained at 37 °C in a humidified atmosphere of 5% CO₂ in air. The medium was changed every third day until confluence, when cell lines were sub-cultured in order to prevent cell death.

To sub-culture, the cell monolayer was washed with phosphate-buffered saline (PBS) (Sigma) and incubated with trypsin/EDTA solution (0.25% trypsin, 1 mM EDTA, Sigma) for 5 min at 37 °C to detach the cells. The effect of trypsin was then inhibited by adding culture medium at room temperature. Cells were used in the fifth passage.

The glass ceramic samples were steam sterilized (120 °C, 20 min), placed in untreated 24-well plates (~2 cm² surface area) to avoid cell adhesion to the bottom of the wells. The cells were seeded at 5×10^4 cells well⁻¹ and 500 μ l fresh medium (supplemented with vitamin C, dexamethasone and β -glycerophosphate) was added, followed by incubation at 37 °C for 4 h to allow cell adhesion. Afterwards, fresh medium was added until it reached a final volume of 2 ml well⁻¹.

HBMSCs were cultured on samples of the glass ceramic for periods of 3, 7, 14 and 21 days. At each time point the samples were evaluated for cell adhesion, distribution and morphology by SEM and cell numbers were quantified by total protein assay. SEM negative and positive controls were prepared using culture medium without cells. For the protein studies a positive control was used employing coverslips in tissue culture polystyrene sheet (TCPS).

2.3.2. Scanning electron microscopy

To dry the specimens for SEM examination two methods were used: critical point drying (CPD) and evaporation of hexamethyldisilazane (HMDS).

Glass ceramic specimens were washed twice with PBS and fixed in a solution of 1.5 vol.% glutaraldehyde and 0.14 M sodium cacodylate (pH 7.4) for 30 min at room temperature. Dehydration was performed by sequential immersion in serial diluted ethanol solutions of 50, 70, 80, 90, 99 and 100 vol.%. The samples were kept in absolute alcohol and taken to critical point using CO₂. The samples were then sputtered with a thin gold film for SEM analysis.

Drying by evaporation of HMDS has been used as an alternative sample preparation to compare the results and avoid interactions due to the preparation method. In this method, once the samples had been dehydrated 100 μ l of HMDS was added drop-wise to the cell area requiring fixation. Then the samples were kept in a hood overnight. After complete evaporation of the HMDS the specimens were sputtered with a thin gold film and visualized by SEM.

2.3.3. Confocal laser scanning microscopy

The glass ceramic specimens were washed twice with PBS, fixed in 3.7 vol.% formaldehyde (10% methanol-free, Polyscience) for

15 min, permeabilized with 0.1 vol.% Triton X-100 for 5 min and incubated in 10 mg ml⁻¹ bovine serum albumin and 10 μ g ml⁻¹ RNase for 60 min at room temperature. F-actin filaments were stained with Alexafluor-conjugated phalloidin (Molecular Probes) for 20 min and nuclei were counterstained with 10 mg ml⁻¹ propidium iodide (Sigma) for 15 min in the dark. Finally, samples were washed with PBS and mounted in Vectashield® and stored in the dark at 2–6 °C. CLSM images were acquired in a Bio-Rad MRC 600 microscope and processed using Leica software.

2.3.4. Total protein content assay

The following procedure was carried out to determine the total protein content. Triton X-100 (1 vol.%) was added to each well and the plates were agitated slightly to spread the Triton in the wells. After 1 min total sonication the plate was removed from the sonicator and homogenized. Then an aliquot from each well was transferred to a microplate reader and bicinchoninic acid (BCA) reagent added. The absorbance in the microplates at 540 nm was then read. A calibration curve was fitted and the protein content per well was calculated. The results of the total protein content assay are shown as the arithmetic means \pm standard deviation. The number of replicates used was five.

3. Results

3.1. Material characterization

Chemical analysis (Table 2) showed that the glass ceramic sample retained a stoichiometric eutectic composition, with no loss of any volatile component. The level of impurities may be considered to be negligible.

The results of qualitative XRD analysis and quantitative Rietveld full-phase analysis (including the amorphous content) of the glass ceramic showed that the phases present in the sample are 44.8(6) wt.% Ca-deficient apatite, 28.0(5) wt.% wollastonite-2M and 27.2(6) wt.% amorphous phase. The overall amorphous phase content of the sample analyzed was derived from the refined CaF₂ internal standard phase ratio. The phase fractions of the crystalline components obtained directly from the Rietveld analysis were normalized by taking into account the overall non-diffracting fraction. The Rietveld plot (15–58°/2 θ) for the glass ceramic is shown in Fig. 1 (the R_{WP} disagreement factor value was less than 10%, indicating a good fit). Furthermore, the values of the phase-dependent disagreement factor (R_F) were quite small, indicating that the fit is very satisfactory [32,33].

The glass ceramic specimens after chemical etching (5 vol.% acetic acid for 1 s) presented a homogeneous microstructure formed of colonies, of around 2 μ m diameter, comprising a mixture of nanometric crystals (~20–50 nm) of a highly chemically etched phase (dark phase in Fig. 2), attributed to Ca-deficient apatite and wollastonite-2M crystals, dispersed in a continuous and interlocked residual amorphous phase (light gray phase).

Prior to exposure to cell culture medium the finished surfaces of the glass ceramic samples obtained were observed by SEM. This revealed a rough surface (Fig. 3).

Table 2
X-ray fluorescence analysis of the glass ceramic.

W-TCP	CaO	SiO ₂	P ₂ O ₅	MgO	Na ₂ O	K ₂ O	Fe ₂ O ₃	MnO	TiO ₂
Experimental ^a	50.7(2)	30.7(3)	18.5(2)	0.10(1)	0.054(3)	0.006(1)	0.036(5)	0.005(1)	0.012(2)
Theoretical	50.7	31.0	18.3						

^a Last digit uncertainties in parentheses.

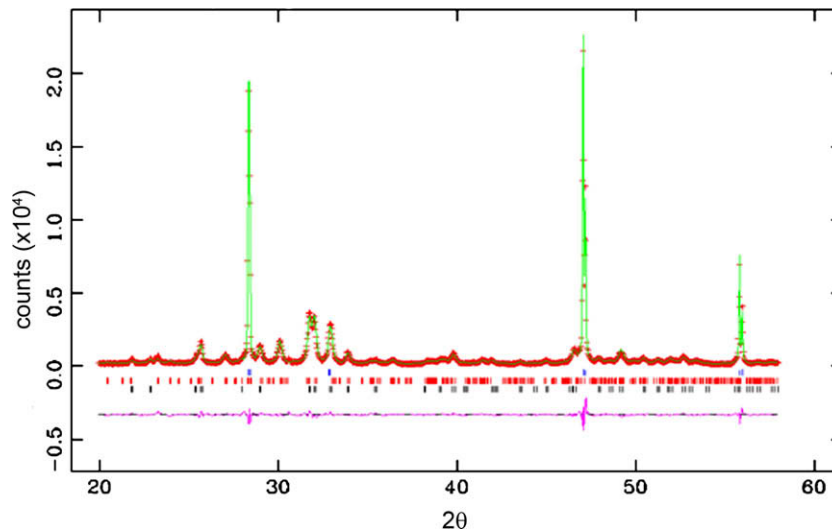


Fig. 1. GSAS Rietveld plot ($15\text{--}58^\circ/2\theta$) for the designed glass ceramic with the peaks of each phase labeled. The marks correspond to the Bragg peaks of the different phases, from bottom to top: Ca-deficient apatite, $\text{CaSiO}_3\text{-}2\text{M}$ and CaF_2 (internal standard). Observed (crosses), calculated (line) and difference (bottom line) powder patterns are shown.

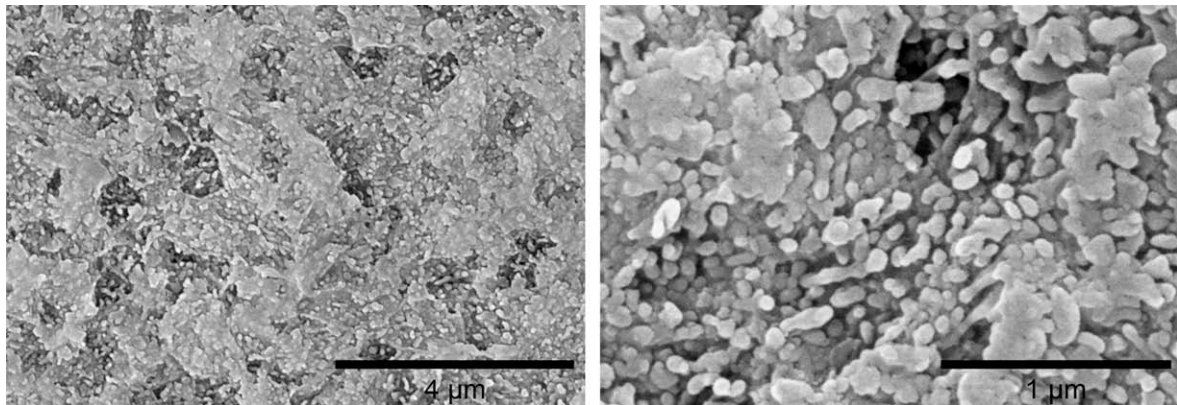


Fig. 2. Chemically etched surface of the glass ceramic. Ca-deficient apatite and wollastonite-2M crystals within an interlocked residual amorphous phase.

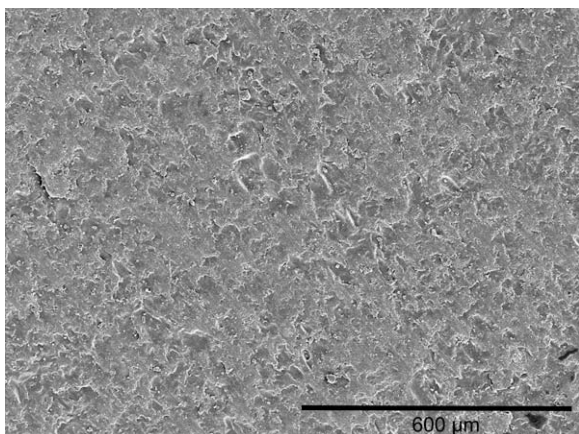


Fig. 3. SEM microphotograph of the glass ceramic surface before exposure to cell culture medium revealing a rough surface.

3.2. Cell morphology and adherence

SEM images (Figs. 4 and 5) show the morphological features of osteoblast-like cells cultured on W-TCP ceramic glass samples for 3, 7, 14 and 21 days, respectively. The cells were observed to ad-

here and spread, forming an intimate contact with the surface of the glass ceramic specimens.

On day 3 of incubation (Figs. 4A and 5A) attached cells showed a typical osteoblast morphology, with a spread polygonal shape and cytoplasmic extensions conforming to the bioactive glass ceramic surface.

On day 7 of incubation (Figs. 4B and 5B) the cells had spread and were in physical contact with each other. The cells formed a dense cell layer, covering the surface of the glass ceramic. Cells cultured on the surface of the W-TCP glass ceramic appeared flat and progressed to a monolayer of cells.

On day 14 of cell culture (Figs. 4C and 5C) cell coverage was greater than on day 7, but it was still possible to see the surface of the material.

In the case of the CPD method, after 21 days incubation (Fig. 4D) the surface was almost totally covered with a heterogeneous layer of cells and it was not possible to see the material surface underneath, since it was completely coated with cells. One could estimate the material surface topography by the way the cells were attached. However, in the sample prepared by the HMDS method (Fig. 5D) the presence of cells on day 21 was not as prominent. This indicates that there were small areas with fewer spreading cells because these areas were not properly seeded. This finding is a good sign, as it indicates that the cells had proliferated easily and were able to move to different areas and start to colonize new regions of the sample.

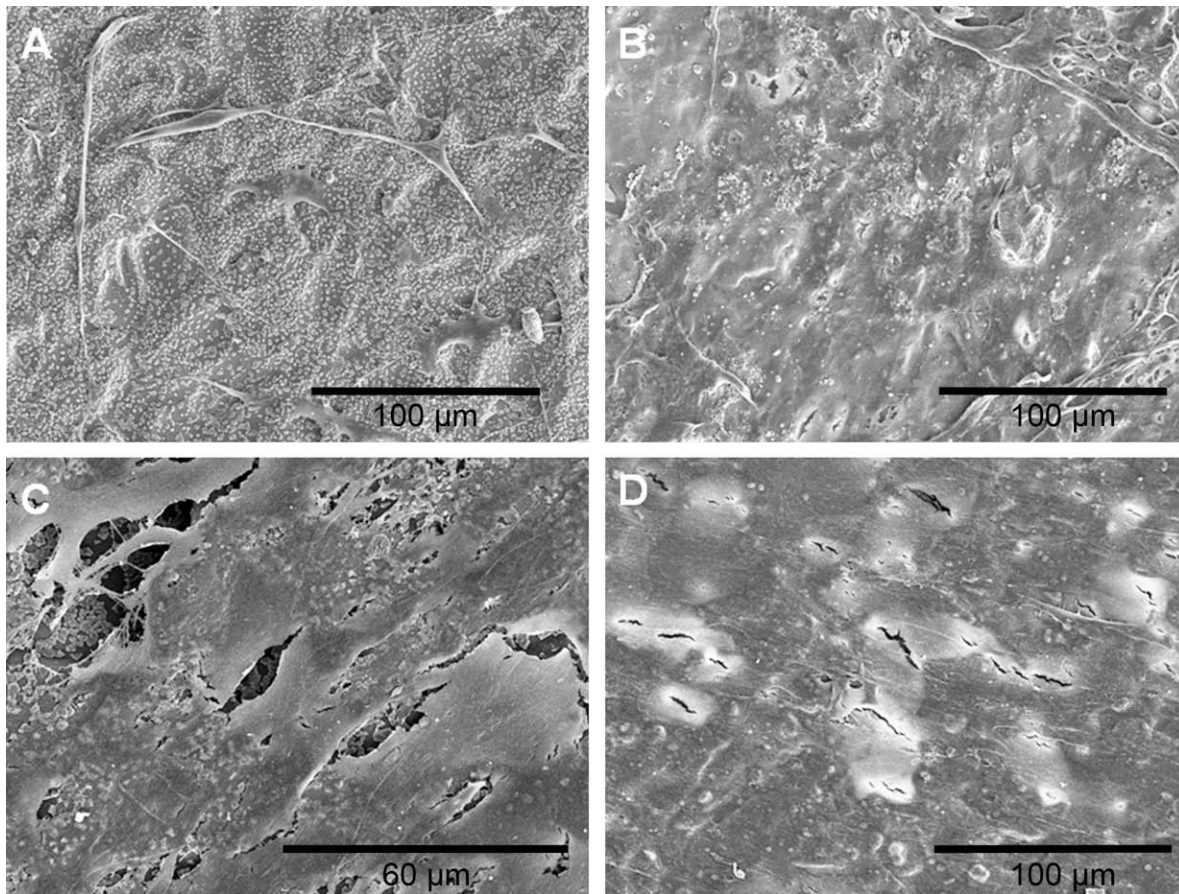


Fig. 4. SEM microphotographs of the glass ceramic treated with CPD for (A) 3, (B) 7, (C) 14 and (D) 21 days of cell culture.

The results obtained by means of the CPD and HMDS methods indicate that similar results can be obtained with both techniques. In the case of the CPD method some ruptured cells were visible, while in the case of the HMDS technique shrinkage of the cells was observed.

Fig. 6 shows one side of a cubic sample after 21 days incubation. Due to the experimental set-up, the sides are less favorable than the top of the sample for cell colonization and proliferation. Hence, in this area fewer cells were observed and the surface of the glass ceramic can be seen. When compared with the original surface, before exposure to cell culture medium (Fig. 3), it became clear that the surface morphology was altered. After 21 days incubation the surface was composed of uniform, $\sim 2 \mu\text{m}$ size, globular structures. EDS microanalysis performed in this area indicated a preponderance of the elements Ca and P (Fig. 6).

CLSM images of the glass ceramic seeded with HBMSCs are shown in Figs. 7 and 8. With this technique it was possible to see that the cells on day 3 (Fig. 7A) were starting to concentrate at specific locations, forming cell clusters. On days 7 (Fig. 7B) and 14 (Fig. 7C) it could be seen that proliferation had increased, confirming the previously presented data. On day 21 the surface of the samples was totally covered with cells (Figs. 7C and 8). This confirmed that the cells were able to adhere and proliferate on the surface of the glass ceramic.

3.3. Total protein content assay

Fig. 9 shows the results for total protein content. It may be seen that the proportion of total protein present in the glass ceramic samples was higher than for the control during the whole experi-

ment. For the last day of study, day 21, the quantity of total protein diminished for the control samples, whereas for the W-TCP samples it kept on increasing. This indicates that the cells on the 21 day control samples had probably reached the stage of differentiation, while those on the W-TCP samples continued to proliferate.

4. Discussion

The glass ceramic obtained in the present work had a fully dense and homogeneous microstructure formed by colonies, of around $2 \mu\text{m}$ in diameter, comprising a mixture of nanometric crystals ($\sim 20\text{--}50 \text{ nm}$) of Ca-deficient apatite and wollastonite-2M crystals within an interlocked residual amorphous phase. This specific micro-nanostructure should improve the mechanical properties of the glass ceramic compared with those of the parent glass [e.g. micro-hardness (H_v) for the glass ceramic was $6.5 \pm 0.3 \text{ GPa}$, for the parent glass $5.1 \pm 0.4 \text{ GPa}$] [34]. Here it should be noted that the glass ceramic processing technique used is a well-known and scalable technology.

In the present work biological responses to the glass ceramic were studied using HBMSCs, which have frequently been used to elucidate the responses of bone cells to biomaterials [35–38].

The glass ceramic obtained presents a bioactive surface that shows formation of a calcium phosphate layer after exposure to a human bone marrow cell culture (Fig 6). This apatite-like layer will play an essential role in primary chemical bonding of the material in the case of implantation into a receptor osseous tissue.

The results obtained for the proliferation and growth of HBMSCs on the glass ceramic proved that after 7 days culture the

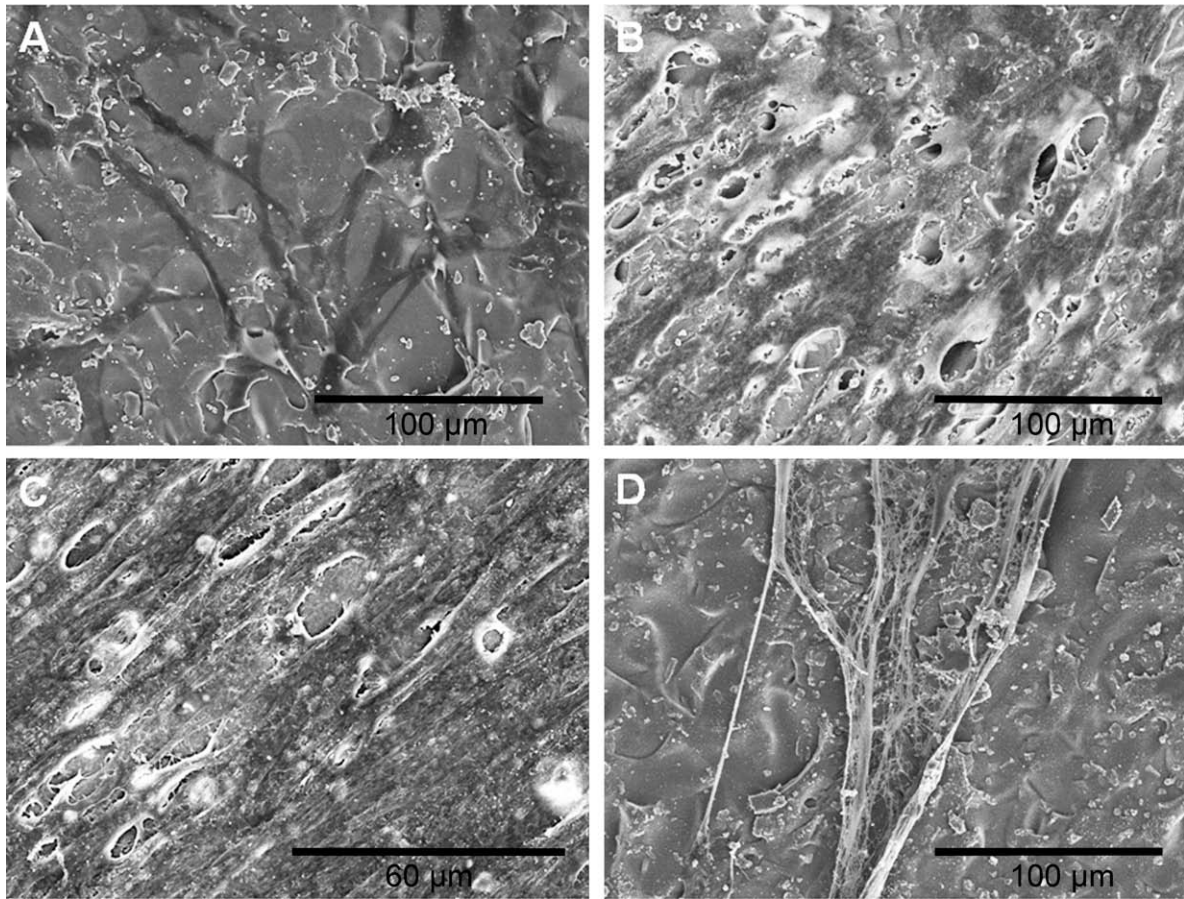


Fig. 5. SEM microphotographs of the glass ceramic treated with HMDS for (A) 3, (B) 7, (C) 14 and (D) 21 days of cell culture.

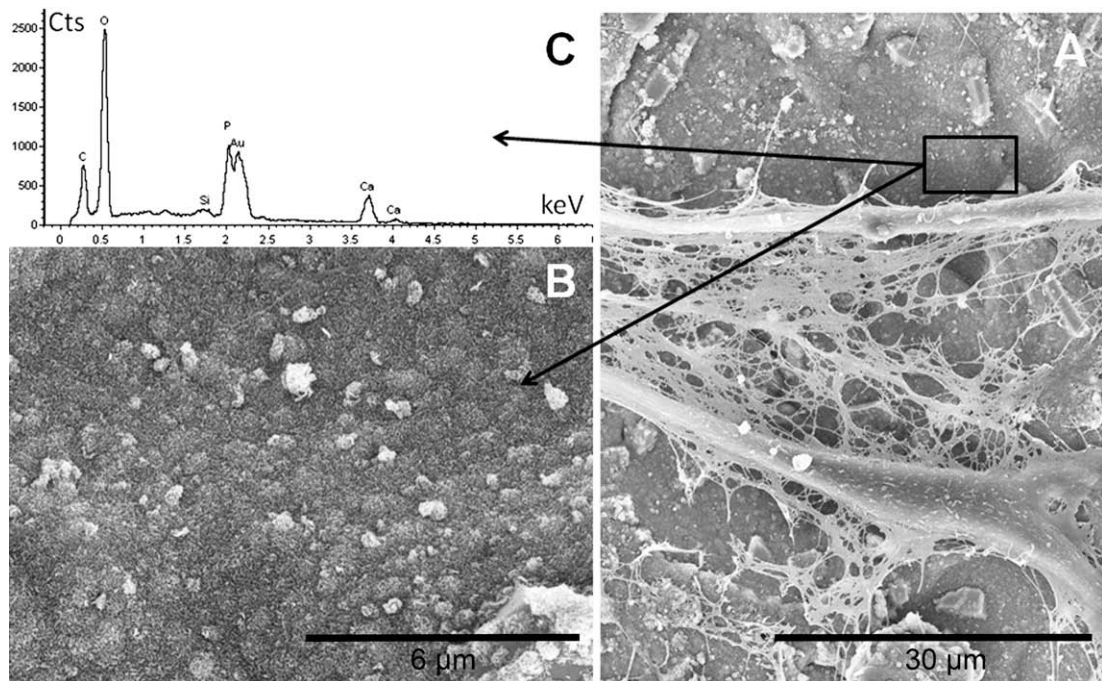


Fig. 6. SEM microphotographs and EDS microanalysis. (A and B) The side of the cubic sample after 21 days incubation. In this area fewer cells are observed and the surface of the glass ceramic can be observed. (C) EDS microanalysis performed on the surface of the glass shows the formation of a calcium phosphate layer by the preponderance of Ca and P elements. The sample was coated with gold. C from the cells was also detected.

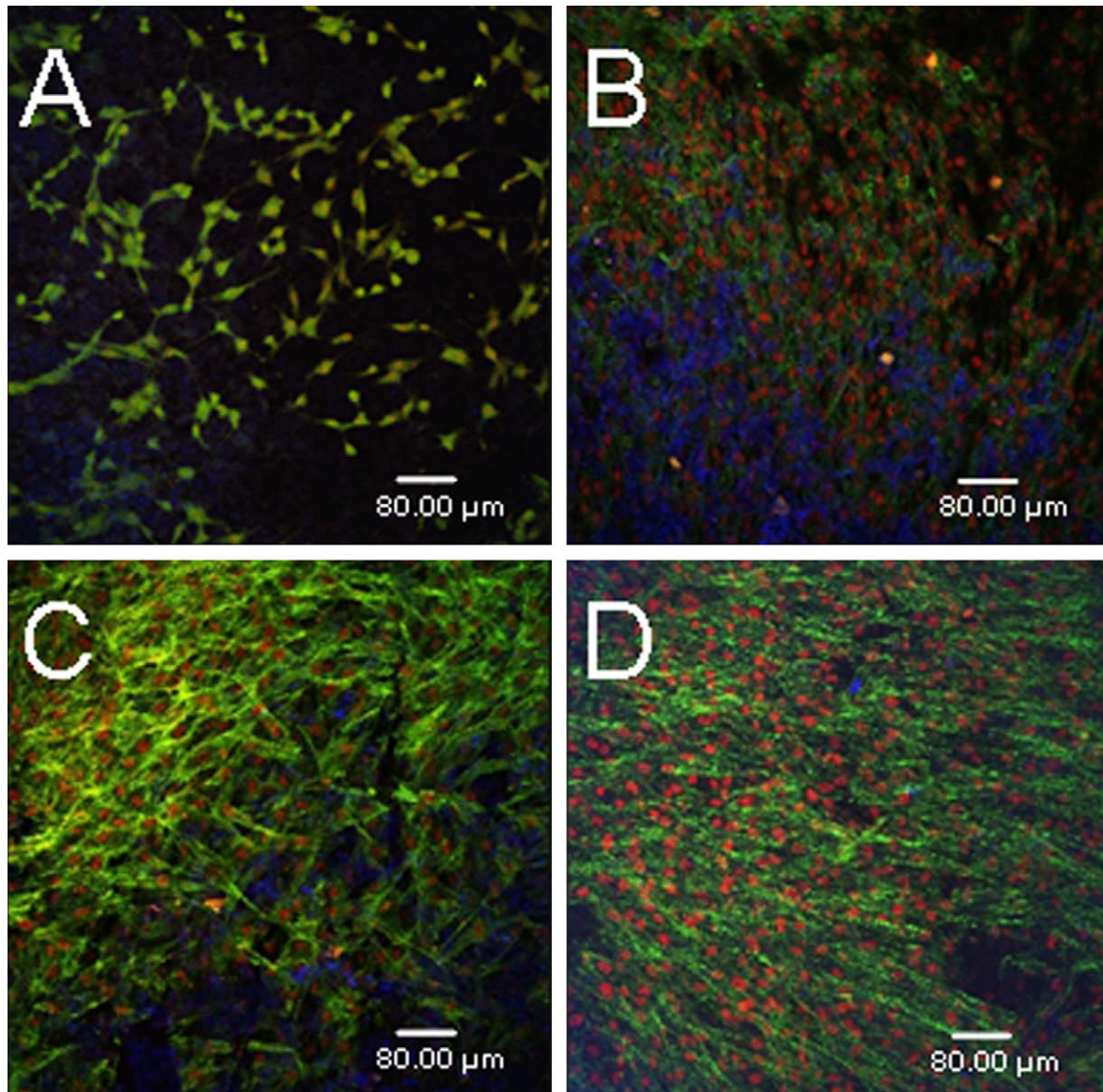


Fig. 7. CLSM of the glass ceramic surface on (A) day 3, (B) day 7, (C) day 14 and (D) day 21. The cell actin filaments are stained green, the nuclei counterstained red.

distribution of cells over the specimens was homogeneous and they were well attached, uniformly colonizing the sample surface. This indicates that the material developed in this study is biocompatible, with a high colonization and proliferation rate.

Several studies [39–41] have shown that surface roughness is an important parameter in basic cell biological responses, improving cell attachment and proliferation. HBMSCs demonstrate significantly higher levels of cell attachment on rough sandblasted surfaces with irregular morphologies than on smooth surfaces [40]. The glass ceramic samples studied in the present work exhibited a rough surface morphology, as shown in Fig. 3. Thus, the surface properties of the material can help to promote osteoblast-like cell attachment.

Cell culture does not allow an analysis of possible differences in response resulting from the different major phases present in the sample (apatite, wollastonite-2M and amorphous phase). Under osteogenic conditions the levels of viable cell adhesion on crack-free specimen surfaces were comparable with other apatite surfaces in osteogenic medium [42].

At this point it is important to note that the inductive effect of the glass ceramic on HBMSCs adhesion and proliferation should be

favorable by the release of Si and Ca ions into the medium and formation of the previously mentioned CaP layer (Fig. 6). These phenomena agree with previous studies of bioactivity in SBF [34]. The glass ceramic exposed to SBF releases Ca and Si ions due to dissolution of the amorphous phase and wollastonite-2M, and finally a CaP layer forms on the surface [34]. Furthermore, different studies have found similar behaviors of materials in SBF and culture medium [36,43,44]. Hence, formation of the CaP layer by release of Ca and Si ions into the medium stimulates osteoblast proliferation.

The present results verify that features such as composition and roughness can modulate cells responses in vitro, including cellular colonization, proliferation, attachment and surface structure of the forming osteoblast multilayer network.

5. Conclusions

Starting from a glass with a stoichiometric eutectic composition within the $\text{Ca}_3(\text{PO}_4)_2$ - CaSiO_3 binary system a new bioglass ceramic has been produced by the introduction of a specific

thermal cycle that allows devitrification of the bulk glass. The resulting crack-free specimens contained 44.8 wt.% Ca-deficient

apatite, 28.0 wt.% wollastonite-2M and 27.2 wt.% amorphous phase.

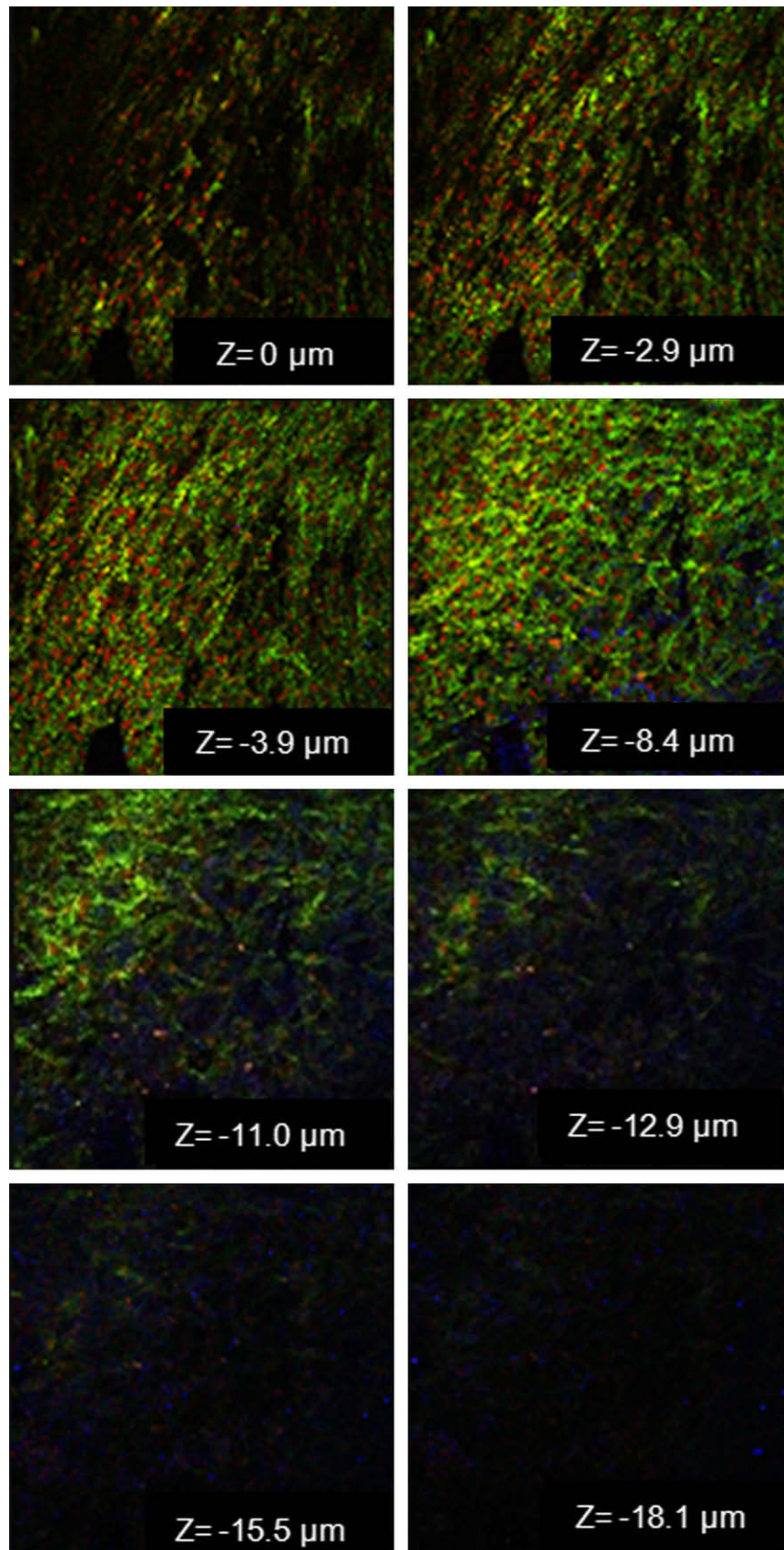


Fig. 8. CLSM of glass ceramic surface on day 21. Z, depth. The cell actin filaments are stained green, the nuclei counterstained red.

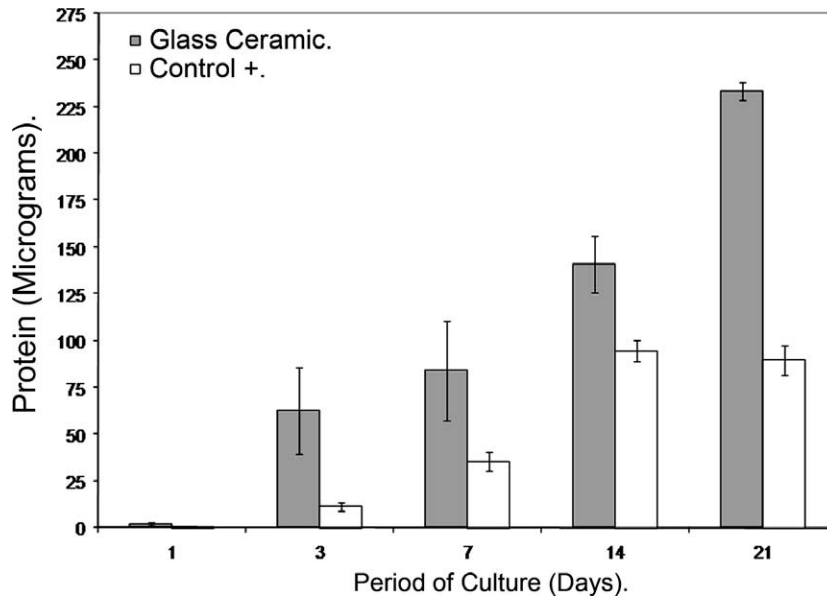


Fig. 9. Total protein content for each period of culture.

The results obtained for the proliferation and growth of human bone marrow cells on the material have proved that the glass ceramic developed in this study is not cytotoxic and cells strongly adhere to the substrate and quickly proliferate on it.

The essential role of co-treatment with silicon and calcium as important elements which enhance HBMSCs activity on phosphate-based biomaterials has been highlighted. Additionally, surface roughness is an important parameter in the basic biological responses, improving cell attachment and proliferation.

The apatite-wollastonite-2M glass ceramic produced could serve as a promising platform for the regeneration of hard tissues.

Acknowledgements

This work was supported by the Science and Technology Inter-Ministry Commission of Spain under project CICYT MAT2006-12749-C02-01. The authors are indebted to the Ministry of Science and Innovation of Spain for its partial support of this work (HP2008-0075) and to the Spanish Research Council (CSIC) for its partial support within the framework of the GRICES/CSIC-2005PT055 cooperation project. M. Magallanes-Perdomo also wishes to acknowledge financial support (MICINN/FPU/AP 2005-5181) from the Ministry of Science and Innovation of Spain.

References

- [1] Hench LL, Wilson J. An introduction to bioceramics. London: World Scientific; 1993.
- [2] Hench LL. Bioceramics: from concept to clinic. *J Am Ceram Soc* 1991;74:1487–510.
- [3] Best SM, Porter AE, Thian ES, Huan J. Bioceramics: past, present and for the future. *J Eur Ceram Soc* 2008;28:1319–27.
- [4] Chevalier J, Gremillard L. Ceramics for medical applications: a picture for the next 20 years. *J Eur Ceram Soc* 2009;29:1245–55.
- [5] Teixeira S, Oliveira S, Ferraz MP, Monteiro FJ. Mesenchymal stem cell proliferation and morphological analysis on interconnected macroporous structures. *Key Eng Mater* 2007;330–332:1129–32.
- [6] Temenoff JS, Mikos AG. Biomaterials: the intersection of biology and materials science. London: Pearson International; 2008. p. 471.
- [7] Carlisle EM. Biochemical and morphological changes associated with long bone abnormalities in silicon deficiency. *J Nutr* 1980;110:1046–55.
- [8] Carlisle EM. A silicon requirement for normal skull formation. *J Nutr* 1980;110:352–9.
- [9] Reffitt M, Ogston N, Jugdaohsingh R, Cheung HF, Evans BA, Thompson RP, et al. Orthosilicic acid stimulates collagen type I synthesis and osteoblastic differentiation in human osteoblast-like cells in vitro. *Bone* 2003;32:127–35.
- [10] Brown L, Luklinska Z, De Aza PN, De Aza S, Anseau M, Hughes FJ, et al. Mechanism of osteoinduction by pseudowollastonite (psW) ceramic. Paper presented at the 7th world biomaterials congress, Sydney; 2004.
- [11] De Aza PN, De Aza AH, De Aza S. Crystalline bioceramic materials. *Bol Soc Esp Ceram V* 2005;44:135–45.
- [12] De Aza PN, De Aza AH, Pena P, De Aza S. Bioactive glasses and glass-ceramics. *Bol Soc Esp Ceram V* 2007;46:45–55.
- [13] Kokubo T, Ito S, Sakka S. Formation of a high-strength bioactive glass-ceramic in the system MgO–CaO–SiO₂–P₂O₅. *J Mat Sci* 1986;21:536–40.
- [14] De Aza PN, Guitián F, De Aza S. Bioeutectic: a new ceramic material for human bone replacement. *Biomaterials* 1997;18:1285–91.
- [15] De Aza PN, Guitián F, De Aza S. A new bioactive material which transforms in situ into hydroxyapatite. *Acta Mater* 1998;46:2541–9.
- [16] De Aza PN, Guitián F, De Aza S. Bioeutectics. International Trademark No. 1.780.697. Universidad de Santiago de Compostela; 1994.
- [17] De Aza PN, Guitián F, De Aza S. Bioeutectics: new bioceramic materials. In: Vicenzini P, editor. *Advances in science and technology. Materials in clinical applications*, vol. 28. Faenza: Publi Techna Italia; 1999. p. 25–32.
- [18] De Aza PN, Luklinska ZB, Anseau MR, Guitián F, De Aza S. Reactivity of wollastonite–tricalcium phosphate ceramic (Bioeutectic®) in parotid human saliva. *Biomaterials* 2000;21:1735–41.
- [19] De Aza AH, Velasquez P, Alemany MI, Pena P, De Aza PN. In situ bone-like apatite formation from a Bioeutectic ceramic in SBF dynamic flow. *J Am Ceram Soc* 2007;90:1200–7.
- [20] Sánchez FM, Díaz-Güemes I, Enciso S, Moreno B, De Aza AH, Carrodegas RG. Evaluación de una cerámica bioactiva de β -wollastonita como sustituto óseo en el modelo ovino. Paper presented at the XVII Congreso Internacional de la Sociedad Española de Cirugía Veterinaria, Cáceres; 6–8 November 2009.
- [21] Llorca J, Orera V. Directionally solidified eutectic ceramic oxides. *Prog Mater Sci* 2006;51:711–809.
- [22] Magallanes-Perdomo M, Carrodegas RG, Pena P, De Aza PN, De Aza S, De Aza AH. Non-isothermal devitrification study of wollastonite–tricalcium phosphate Bioeutectic® glass. *Key Eng Mat* 2009;396–398:127–30.
- [23] Magallanes-Perdomo M, Pena P, De Aza PN, Carrodegas RG, Rodríguez MA, Turrillas X, et al. Devitrification studies of wollastonite–tricalcium phosphate eutectic glass. *Acta Biomater* 2009;5:3057–66.
- [24] De Aza PN, Guitián F, De Aza S. Phase diagram of wollastonite–tricalcium phosphate. *J Am Ceram Soc* 1995;78:1653–6.
- [25] Young RA. The Rietveld method. Oxford: Oxford University Press; 1993. p. 336.
- [26] Larson AC, Von Dreele RB. Los Alamos National Laboratory Report No. LA-UR-86-748. Los Alamos, NM: Los Alamos National Laboratory; 1994.
- [27] Finger LW, Cox DE, Jephcoat AP. A correction for powder diffraction peak asymmetry due to axial divergence. *J Appl Cryst* 1994;27:892–900.
- [28] Wilson RM, Elliott JC, Dowker SE, Rodríguez-Lorenzo LM. Rietveld refinements and spectroscopic studies of the structure of Ca-deficient apatite. *Biomaterials* 2005;26:1317–27.
- [29] Wilson RM, Elliott JC, Dowker SE, Rodríguez-Lorenzo LM. Ca_{9.303}(PO₄)₆(OH)_{0.696}·1.97(H₂O). ICSD collection code 152190, inorganic crystal structure database. Karlsruhe: Fachinformationszentrum; 2005.
- [30] Trojer FJ. The crystal structure of parawollastonite. *Zeitschrift Fur Kristallographie Kristallgeometrie Kristallphysik Kristallchemie* 1968;127:291–308.
- [31] Trojer FJ. CaSiO₃–wollastonite-2M. ICSD collection code 34908, inorganic crystal structure database. Karlsruhe: Fachinformationszentrum; 1968.

- [32] De La Torre AG, Bruque S, Aranda MAG. Rietveld quantitative amorphous content analysis. *J Appl Cryst* 2001;34:196–202.
- [33] De Aza AH, De La Torre AG, Aranda MAG, Valle FJ, De Aza S. Rietveld quantitative analysis of Buen Retiro porcelains. *J Am Ceram Soc* 2004;87:449–54.
- [34] Magallanes-Perdomo M, Luklinska ZB, De Aza AH, Carrodegua RG, De Aza S, Pena P. Bone like apatite forming ability of apatite–wollastonite glass ceramic. Paper presented at the 11th international conference and exhibition of the European ceramic society, Krakow, Poland; 21–25 June 2009.
- [35] Ferraz MP, Fernandes MH, Santos JD, Monteiro FJ. HA and double-layer HA-P₂O₅/CaO glass coatings: influence of chemical composition on human bone marrow cells osteoblastic behavior. *J Mater Sci Mater Med* 2001;12:629–38.
- [36] Meseguer-Olmo L, Bernabeu-Esclapez A, Ros-Martinez E, Sanchez-Salcedo S, Padilla S, Martin AI, et al. In vitro behaviour of adult mesenchymal stem cells seeded on a bioactive glass ceramic in the SiO₂–CaO–P₂O₅ system. *Acta Biomater* 2008;4:1104–13.
- [37] Muller P, Bulnheim U, Diener A, Luthen F, Teller M, Klinkenberg ED, et al. Calcium phosphate surfaces promote osteogenic differentiation of mesenchymal stem cells. *J Cell Mol Med* 2008;12:281–91.
- [38] Saldana L, Sanchez-Salcedo S, Izquierdo-Barba I, Bensiamar F, Munuera L, Vallet-Regi M, et al. Calcium phosphate-based particles influence osteogenic maturation of human mesenchymal stem cells. *Acta Biomater* 2009;5:1294–305.
- [39] Martin JY, Schwartz Z, Hummert TW, Schraub DM, Simpson J, Lankford J, et al. Effect of titanium surface-roughness on proliferation, differentiation, and protein-synthesis of human osteoblast-like cells (MG63). *J Biomed Mater Res* 1995;29:389–401.
- [40] Bowers KT, Keller JC, Randolph BA, Wick DG, Michaels CM. Optimization of surface micromorphology for enhanced osteoblast responses in vitro. *Int J Oral Maxillofac Implants* 1992;7:302–10.
- [41] Boyan BD, Batzer R, Kieswetter K, Liu Y, Cochran DL, Szmuckler-Moncler S, et al. Titanium surface roughness alters responsiveness of MG63 osteoblast-like cells to 1 alpha,25-(OH)(2)D-3. *J Biomed Mater Res* 1998;39:77–85.
- [42] Mateus AYP, Barrias CC, Ribeiro C, Ferraz MP, Monteiro FJ. Comparative study of nanohydroxyapatite microspheres for medical applications. *J Biomed Mater Res A* 2008;86:483–93.
- [43] Ni SY, Chang J, Chou L, Zhai WY. Comparison of osteoblast-like cell responses to calcium silicate and tricalcium phosphate ceramics in vitro. *J Biomed Mater Res B Appl Biomater* 2007;80:174–83.
- [44] Sarmento C, Luklinska ZB, Brown L, Anseau M, De Aza PN, De Aza S, et al. In vitro behavior of osteoblastic cells cultured in the presence of pseudowollastonite ceramic. *J Biomed Mater Res A* 2004;69A:351–8.